

High-fat diet decreases energy expenditure and expression of genes controlling lipid metabolism, mitochondrial function and skeletal system development in the adipose tissue, along with increased expression of extracellular matrix remodelling- and inflammation-related genes

Myung-Sook Choi^{1,2†}, Young-Je Kim^{1†}, Eun-Young Kwon², Jae Young Ryoo³, Sang Ryong Kim³ and Un Ju Jung^{2*}

¹Department of Food Science and Nutrition, Kyungpook National University, 1370 San-Kyuk Dong Puk-Ku, Daegu 702-701, Republic of Korea

²Center for Food and Nutritional Genomics Research, Kyungpook National University, 1370 San-Kyuk Dong Puk-Ku, Daegu 702-701, Republic of Korea

³School of Life Sciences, BK21 Plus KNU Creative BioResearch Group, Kyungpook National University, 1370 San-Kyuk Dong Puk-Ku, Daegu 702-701, Republic of Korea

(Submitted 13 August 2014 – Final revision received 13 November 2014 – Accepted 22 December 2014 – First published online 6 March 2015)

Abstract

The aim of the present study was to identify the genes differentially expressed in the visceral adipose tissue in a well-characterised mouse model of high-fat diet (HFD)-induced obesity. Male C57BL/6J mice (n 20) were fed either HFD (189% of energy from fat) or low-fat diet (LFD, 42% of energy from fat) for 16 weeks. HFD-fed mice exhibited obesity, insulin resistance, dyslipidaemia and adipose collagen accumulation, along with higher levels of plasma leptin, resistin and plasminogen activator inhibitor type 1, although there were no significant differences in plasma cytokine levels. Energy intake was similar in the two diet groups owing to lower food intake in the HFD group; however, energy expenditure was also lower in the HFD group than in the LFD group. Microarray analysis revealed that genes related to lipolysis, fatty acid metabolism, mitochondrial energy transduction, oxidation–reduction, insulin sensitivity and skeletal system development were down-regulated in HFD-fed mice, and genes associated with extracellular matrix (ECM) components, ECM remodelling and inflammation were up-regulated. The top ten up- or down-regulated genes include *Acsm3*, *mt-Nd6*, *Fam13a*, *Cyp2e1*, *Rgs1* and *Gpmb*, whose roles in the deterioration of obesity-associated adipose tissue are poorly understood. In conclusion, the genes identified here provide new therapeutic opportunities for prevention and treatment of diet-induced obesity.

Key words: High-fat diet: Energy expenditure: Global gene expression in adipose tissue: Inflammation

Obesity is one of the major underlying causes of the metabolic syndrome, including insulin resistance, type 2 diabetes and dyslipidaemia. Although the exact mechanisms by which obesity induces or worsens the metabolic risk factors are still unknown, excess adiposity, particularly visceral fat accumulation, is associated with insulin resistance and abnormal glucose and lipid metabolisms⁽¹⁾. In addition, chronic low-grade inflammation in the adipose tissue contributes to the pathogenesis of insulin resistance and metabolic syndrome⁽¹⁾.

Diet composition plays an important role in the development of obesity and its associated metabolic diseases⁽²⁾.

Dietary fat is the most energy-dense macronutrient and causes less satiety than carbohydrate or protein⁽²⁾. Prolonged ingestion of high-fat diet (HFD) has been found to induce hyperphagia, body-weight gain and fat deposition and increase the levels of circulating glucose, insulin and TAG in rats^(3–5). However, results have been inconsistent, with some studies reporting that HFD did not cause hyperphagia, hypertriglycerolaemia, hyperglycaemia or hyperinsulinaemia in mice^(6,7).

Carbohydrates, especially simple sugars, also seem to be associated with obesity and metabolic syndrome. Long-term ingestion of a sugar-rich diet increases fat mass without

Abbreviations: ECM, encoding extracellular matrix; GPCR, G-protein-coupled receptors; HFD, high-fat diet; HOMA-IR, homeostatic index of insulin resistance; LFD, low-fat diet; RGS, regulators of G protein signalling; WAT, white adipose tissue.

* **Corresponding author:** Dr U. J. Jung, fax +82 53 958 1230, email jungunju@naver.com

† These authors contributed equally to this work.

a concomitant increase in energy intake⁽⁸⁾ and promotes insulin resistance in rats⁽⁹⁾. Furthermore, a low-fat, high-carbohydrate diet had deleterious effects on cardiovascular health in obese adults compared with a high-fat, low-carbohydrate diet⁽¹⁰⁾. In contrast, another study has shown that a high-fat, low-carbohydrate diet decreases serum TAG levels and increases serum HDL-cholesterol levels in obese subjects, without concomitant changes in body weight or composition, in comparison with a low-fat, high-carbohydrate diet⁽¹¹⁾. These results show that the role of diet in obesity varies with diet composition, animal species and experimental protocol.

Recently, nutritional genomics studies have analysed the responses of tissues to different diets and nutrients in order to provide a insight into the molecular events underlying diet-induced obesity⁽¹²⁾. However, obesity-related metabolic and molecular changes in response to HFD (containing low carbohydrate) *v.* low-fat diet (LFD; containing high carbohydrate) are not yet fully understood. Moreover, the HFD used in most animal studies of diet-induced obesity contains an extremely high fat content (approximately 60% of total energy)⁽¹¹⁾, which does not mimic the moderate fat content of Western human diets (approximately 40–45% of total energy).

Therefore, the primary aim of the present study was to compare the effects of long-term ingestion of HFD (189% of energy from fat) and LFD (which provides more carbohydrate, namely maize starch and sugar) on food intake, energy expenditure, body weight and adiposity, as well as plasma glucose, insulin, lipid and adipocytokine profiles, in C57BL/6J mice. The secondary aim of the present study was to obtain a further insight into the molecular mechanisms underlying the development of diet-induced obesity and its related metabolic abnormalities in response to HFD and to identify differentially expressed genes in the epididymal white adipose tissue (WAT) of HFD-fed mice using microarray analysis.

Experimental methods

Feeding protocol, energy expenditure and blood biomarkers

Male C57BL/6J mice (4-week old) were purchased from Jackson Laboratories and individually housed at room temperature on a 12h light–12h dark cycle. After 1 week of acclimation, they were fed a LFD (D12450B, 16.17 kJ/g; Research Diets) or a HFD (D12451, 19.866 kJ/g; Research Diets) *ad libitum* for 16 weeks. The LFD contains 42% of energy from fat (25.2% of energy from soyabean oil and 16.8% of energy from lard), 29.4% of energy from carbohydrate (130.2% of energy from maize starch, 16.8% of energy from maltodextrin and 14.7% of energy from sucrose) and 84% of energy from protein, whereas the HFD contains 189% of energy from fat (25.2% of energy from soyabean oil and 163.8% of energy from lard), 14.7% of energy from carbohydrate (29.4% of energy from maize starch, 4.2% of energy from maltodextrin and 75.6% of energy from sucrose) and 84% of energy from protein. Food intake of each mouse

was measured daily throughout the study by subtracting the remaining food from the amount of food given to the mice, and daily food intake was calculated from the averaged food intake throughout the study. Energy expenditure for 24 h was measured at 14 weeks of feeding on the experimental diets using an indirect calorimeter (Oxylet; Panlab). Mice were killed as described previously⁽⁶⁾, and epididymal WAT, perirenal WAT, retroperitoneal WAT, mesenteric WAT and subcutaneous WAT were promptly removed, rinsed with physiological saline and weighed after blood collection. Among them, the epididymal WAT, which is widely used for the metabolic study due to its anatomically distinct feature, relative abundance and metabolic sensitivity^(13–18), was immediately fixed in 10% buffered formalin for morphological examination and was frozen in liquid N₂ and stored at –70°C until RNA analysis. Plasma concentrations of NEFA, phospholipid (Wako Chemicals), TAG, total cholesterol and HDL-cholesterol (Asan Pharmaceutical Co., Ltd) were determined using commercially available kits.

Plasma adipocytokine and insulin levels were determined using a multiplex detection kit (Bio-Rad) and analysed using a Luminex 200 Labmap system. Fasting blood glucose concentration was measured using a glucose analyser (Glucocard; Arkray), and the homeostatic index of insulin resistance (HOMA-IR) was calculated as (fasting glucose (mmol/l) × fasting insulin (pmol/l)/135). All the experimental procedures were approved by the Kyungpook National University Ethics Committee (Approval no. KNU-2011-49).

Morphology of the epididymal white adipose tissue

The epididymal WAT was fixed in 10% buffered formalin. Fixed tissues were embedded in paraffin, and 4 µm sections were prepared and stained with haematoxylin and eosin and Masson's trichrome. The stained areas were viewed using an optical microscope (Nikon) with a magnification of 200 ×, and epididymal adipocyte size and fibrotic area from the Masson's trichrome staining were measured by computer analysis using the Leica Application Suite (version 2.8.1; Leica Microsystems).

RNA isolation, microarray analysis and real-time quantitative PCR

Total RNA was extracted from the epididymal WAT using TRIzol reagent (Invitrogen Life Technologies). For quality control, RNA purity and integrity were assessed using an Agilent 2100 Bioanalyzer (Agilent Technologies). Three pooled RNA sample sets were constructed to represent the LFD and HFD groups, as described previously⁽¹⁹⁾.

For microarray analysis, total RNA was amplified and purified using an Illumina RNA amplification kit (Ambion[®]) and quantified using an ND-1000 spectrophotometer (NanoDrop). Biotinylated cRNA (750 ng) was hybridised to MouseWG-6 v2.0 Expression BeadChips (Illumina, Inc.) at 58°C for 16–18 h. Array signal detection was carried out using Amersham Cy3-streptavidin (GE Healthcare Bio-Sciences). BeadChips were scanned using an Illumina BeadArray Reader, and raw data



were extracted using the Illumina BeadStudio software. Probe signal intensities were quantile-normalised and log-transformed. Limma was used to determine significantly differentially expressed genes based on a false discovery rate less than 5%, a Benjamin and Hochberg-adjusted P value <0.05 and a \log_2 fold change greater than 1⁽¹⁹⁾. The DAVID Functional Annotation Tool was used to identify the enriched biological themes and cluster-redundant annotation terms. These microarray data were deposited in Gene Expression Omnibus database (accession no. GSE63198).

To validate microarray data, several differentially expressed genes (*Rgs1*, *Mmp2*, *Ccl2*, *Tlr2*, *Tlr4* and *Irs2*) were measured independently by real-time quantitative PCR using the same pooled RNA samples that were hybridised to BeadChips. Total RNA (1 μg) was reverse-transcribed into complementary DNA using a QuantiTect reverse transcription kit (Qiagen), and real-time quantitative PCR was carried out on a CFX96 real-time system (Bio-Rad) using a SYBR Green PCR kit (Qiagen). Values were normalised to glyceraldehyde-3-phosphate dehydrogenase levels, and relative gene expression was calculated by the $2^{-\Delta\Delta Ct}$ method.

For definition of gene abbreviations, see online Supplementary Table S1.

Statistical analyses

All data are presented as means with their standard errors. Statistical analyses were performed using SPSS software. Changes in body weight were analysed by repeated-measures ANOVA, and other data were analysed by Student's t test or Wilcoxon t test. Results were considered statistically significant when $P < 0.05$.

Results

High-fat diet decreased food intake but increased body weight and fat mass by decreasing energy expenditure

HFD-fed mice exhibited a significantly greater body weight than LFD-fed mice, although the average daily food intake throughout the study was markedly lower in HFD-fed mice and the average daily energy intake did not differ between the two groups (Fig. 1(a)–(c)). Interestingly, indirect calorimetry revealed that HFD-fed mice had lower energy expenditure than LFD-fed mice (Fig. 1(d)). As expected, the subcutaneous WAT and the visceral WAT (including epididymal, perirenal, retroperitoneal and mesenteric WAT) weights, adipocyte size and adipose collagen accumulation were higher in HFD-fed mice (Fig. 1(e) and (f)).

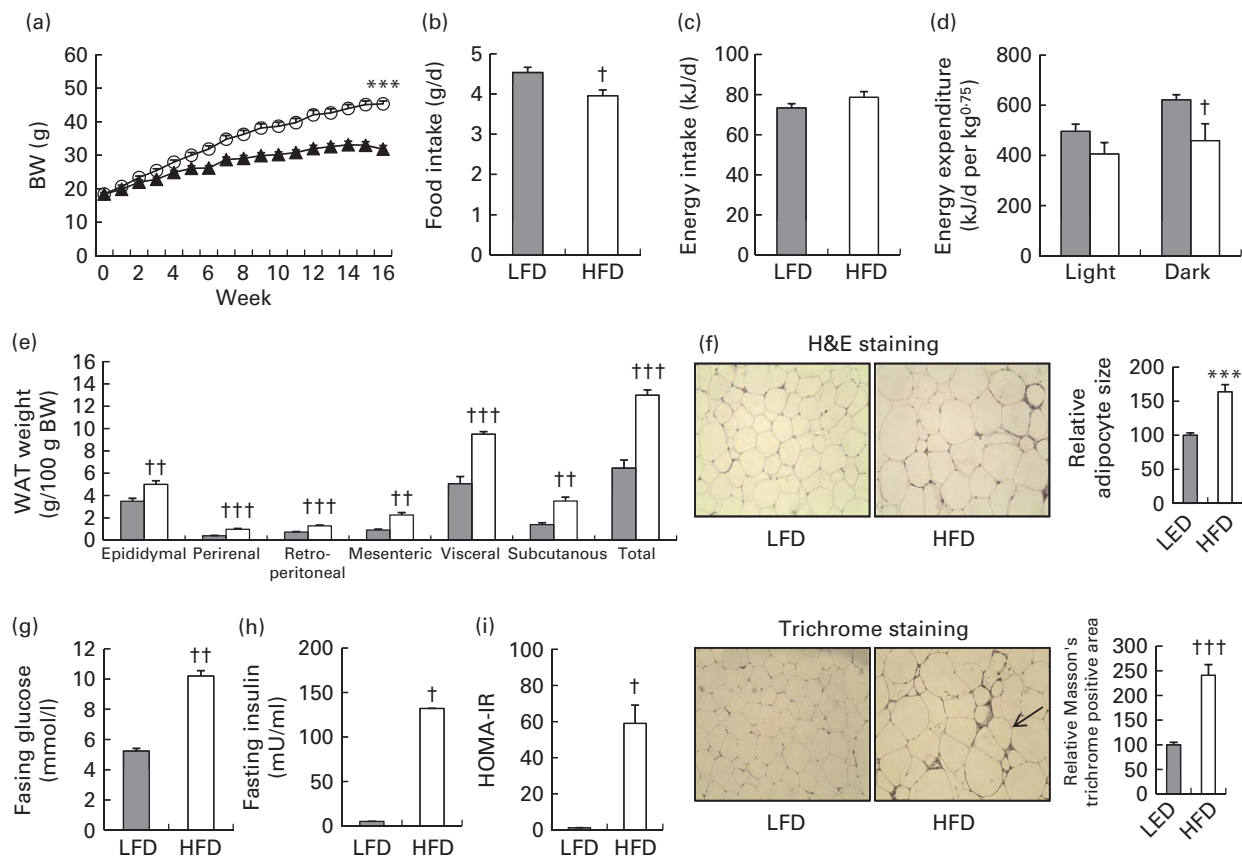


Fig. 1. Metabolic and morphological phenotype of high-fat diet (HFD, \circ , \square)-fed mice. Values are means with their standard errors represented by vertical bars (n 10). (a) *** Mean value was significantly different from that of low-fat diet (LFD, \blacktriangle) group ($P < 0.001$; repeated-measures ANOVA). (b–i) Mean value was significantly different from that of low-fat diet (LFD, \blacksquare) group: $\dagger P < 0.05$, $\ddagger P < 0.01$, $\ddagger\ddagger P < 0.001$ (Student's t test). (f) Representative photographs of adipocytes in the epididymal white adipose tissue (WAT) of mice at $\times 200$ magnification (left panel) and quantitative analysis (right panel). The WAT section stained with Masson's trichrome showed significant deposition of collagens, primarily collagen I and III (blue stain indicated with arrowheads), in HFD-fed mice. BW, body weight; H&E, haematoxylin and eosin; HOMA-IR, homeostatic index of insulin resistance. (A colour version of this figure can be found online at <http://www.journals.cambridge.org/bjn>)

Table 1. Plasma adipocytokine and lipid levels (Mean values with their standard errors; *n* 10)

	LFD		HFD	
	Mean	SE	Mean	SE
Adipocytokines				
Leptin (ng/ml)	2.83	0.79	57.13***	6.11
Resistin (ng/ml)	208.74	32.04	575.91***	23.79
PAI-1 (ng/ml)	1.26	0.74	2.42**	0.32
Adiponectin (μg/ml)	11.38	1.27	13.43	0.66
MCP-1 (pg/ml)	248.44	26.69	234.71	30.12
TNF-α (pg/ml)	2016.99	267.50	1633.68	275.39
IL-6 (pg/ml)	23.36	3.05	22.74	3.66
IL-10 (pg/ml)	920.36	93.69	850.00	85.90
Lipids				
NEFA (mmol/l)	0.90	0.07	0.91	0.07
TAG (mmol/l)	0.81	0.08	1.04	0.07
Phospholipid (mmol/l)	0.92	0.15	2.45*	0.15
Total cholesterol (mmol/l)	2.61	0.28	4.34**	0.32
HDL-cholesterol (mmol/l)	1.35	0.19	1.98*	0.18
Atherosclerotic index	1.26	0.33	1.26	0.19

LFD, low-fat diet; HFD, high-fat diet; PAI-1, plasminogen activator inhibitor type 1; MCP, monocyte chemoattractant protein.

Mean values were significantly different from those of the LFD group: **P*<0.05, ***P*<0.01, ****P*<0.001.

High-fat diet induced hyperglycaemia, hyperinsulinaemia and insulin resistance

Fasting blood glucose level was significantly increased in HFD-fed mice (Fig. 1(g)). HFD also resulted in significant increases in plasma insulin level and HOMA-IR compared with LFD (Fig. 1(h) and (i)).

High-fat diet increased plasma leptin, resistin and plasminogen activator inhibitor type 1 levels but did not alter plasma adiponectin and cytokine levels

Plasma leptin, resistin and plasminogen activator inhibitor type 1 levels were significantly higher in HFD-fed mice than in LFD-fed mice (Table 1). However, there was no significant difference in plasma adiponectin level between the two groups. The levels of plasma cytokines (monocyte chemoattractant protein 1, TNF-α, IL-6 and IL-10) were also not significantly altered by HFD.

High-fat diet increased plasma phospholipid, total cholesterol and HDL-cholesterol levels but did not alter plasma NEFA and TAG levels

No significant differences in plasma NEFA or TAG levels were observed between the HFD and LFD groups (Table 1). However, plasma phospholipid level was significantly higher in HFD-fed mice. HFD also increased plasma total cholesterol

level, as well as HDL-cholesterol level, resulting in no significant difference in atherogenic index between the two groups.

Gene expression profiles in the epididymal white adipose tissue

To determine the changes in global gene expression profiles of the epididymal WAT in HFD-induced obesity, we identified differentially expressed genes in HFD-fed mice compared with LFD-fed mice using microarray analysis. Of the 45 000 analysed expression probes, 1270 were different between the two groups. Among these 1270 HFD-responsive genes, 657 were up-regulated and 397 were down-regulated. The top ten differentially expressed genes are listed in Table 2. Functional annotation clustering using DAVID revealed that the majority of genes up-regulated by HFD were related to immune and inflammatory responses (Table 3; online Supplementary Table S2). These included genes encoding chemokines, receptors of chemokines and cytokines, toll-like receptors, C-type lectin receptors, Fc receptors and surface markers of immune cells (Table 4). Moreover, HFD induced up-regulation of genes encoding extracellular matrix (ECM) components such as collagen (*Col1a1*, *Col3a1*, *Col5a2*, *Col6a2* and *Col6a3*), glycosaminoglycan and proteoglycan (*Sdcbp* and *Lum*), adhesive glycoproteins (*Mfap5*, *Gpnmb* and *Fn1*) and integrin (*Itgad*, *Itgam* and *Itgax*), as well as genes encoding proteins involved in ECM remodelling and regulation, such as cathepsins (*Ctsa*, *Ctsb*, *Ctsk*, *Ctsl*, *Ctss* and *Ctssz*), a disintegrin and metalloprotease (ADAM) domain (*Adam8*, *Adam12* and *Adam17*), matrix metalloproteinases (MMP: *Mmp2*, *Mmp3*, *Mmp12* and *Mmp13*), tissue inhibitors of metalloproteinases (*Timp1*) and other fibrosis-related genes (*Tgfb1*). Interestingly, the expression of two ADAM and MMP genes, *Adam7* and *Mmp9*, was down-regulated in obesity.

The genes that were down-regulated in response to HFD were enriched in gene ontology categories related to oxidation–reduction, fatty acid metabolism, insulin response and skeletal system development (Table 3; online Supplementary Table S2). Down-regulated genes related to oxidation–reduction included genes controlling antioxidant defence (*Gpx3*), detoxification (*Aldb1a1*, *Aldb6a1*, *Cyp2d9*, *Cyp2d22*, *Cyp2e1*, *Cyp2f2*, *Gsta3* and *Gsta4*) and mitochondrial energy transduction pathways such as the TCA cycle (*Por*) and oxidative phosphorylation (*Ndufb4* and *Ndufb9*) (Table 4). HFD decreased the expression of genes involved in lipolysis, thermogenesis (*Adrb3*) and fatty acid uptake, transport (*Fabp4*, *Cd36* and *Slc27a2*), elongation (*Elavl6*), activation and oxidation (*Acsm3*, *Acacb*, *Acot4*, *Acadslb*, *Hadh* and *Faah*). Consistent with increased insulin resistance,

Table 2. Top ten differentially expressed genes in the epididymal white adipose tissue of high-fat diet-fed mice

Differentially expressed genes*	
Up-regulated genes	<i>Rgs1</i> , <i>Mmp12</i> , <i>Gpnmb</i> , <i>Trem2</i> , <i>Tph2</i> , <i>Saa3</i> , <i>Ubd</i> , <i>Atf3</i> , <i>Itgad</i> , <i>Cd68</i>
Down-regulated genes	<i>Acsm3</i> , <i>Pck1</i> , <i>Fabp4</i> , <i>LOC384538</i> , <i>mt-Nd6</i> , <i>Ffar3</i> , <i>1810022C23Rik</i> , <i>Fam13a</i> , <i>Cyp2e1</i> , <i>scl33870-2_144</i>

* Differentially expressed genes were determined using Limma in R/Bioconductor, based on *P*<0.05, false discovery rate <5% and log₂ fold change >1. For definition of gene abbreviations, see online Supplementary Table S1.

Table 3. Functional annotation clusters of up-regulated and down-regulated genes in the epididymal white adipose tissue of high-fat diet-fed C57BL/6J mice*

ES	Function	Count	P
Up-regulated genes			
13.67	Immune response	63	7.00×10^{-21}
	Inflammatory response	39	4.10×10^{-16}
	Response to wounding	47	3.70×10^{-15}
	Defence response	49	9.30×10^{-13}
	Cell activation	38	1.20×10^{-14}
6.21	Cell proliferation	20	9.80×10^{-04}
	Chemotaxis/taxis	22	1.30×10^{-10}
5.94	Positive regulation of immune response	23	6.90×10^{-10}
5.09	Positive regulation of response to stimulus	24	7.90×10^{-08}
4.64	Regulation of cytokine production	24	3.40×10^{-10}
4.02	Phagocytosis	12	5.40×10^{-07}
3.95	Cell division	25	5.70×10^{-05}
3.14	Cell cycle	41	9.00×10^{-05}
	Positive regulation of immune system process	33	3.20×10^{-13}
2.68	Negative regulation of immune system process	12	4.80×10^{-05}
Down-regulated genes			
4.71	Oxidation–reduction	36	1.90×10^{-07}
4.44	Fatty acid metabolism	19	1.40×10^{-07}
2.42	Response to insulin stimulus	9	5.40×10^{-04}
2.08	Skeletal system development and morphogenesis	17	8.80×10^{-06}
	Pattern specification process	16	1.60×10^{-04}

ES, enrichment score.

*Functional annotation terms were clustered according to biological processes.

insulin sensitivity-related genes, such as those encoding insulin receptor substrate 2 (*Irs2*) and GLUT 3 (*Slc2a3*), were down-regulated by HFD feeding. Along with *Mmp9*, multiple genes controlling skeletal system development and pattern specification (*Bmp4*, *Hoxa5*, *Hoxa7*, *Hoxb5*, *Hoxc6*, *Irx3* and *Igf2*) were also down-regulated in HFD-fed mice. The expression of many genes encoding G-protein-coupled receptors (GPCR: *Gpr64*, *Gpr120*, *Gpr109a*, *Gpr156* and *Opn3*) was decreased in response to HFD, whereas mRNA expression of regulators of G protein signalling (RGS: *Rgs1* and *Rgs10*) was increased. Several genes identified as differentially expressed based on microarray analysis were independently validated by real-time quantitative PCR (Fig. 2).

Discussion

It is generally accepted that HFD induces hyperphagia, and that increased energy intake is the major mechanism by which HFD causes obesity^(2,3). In the present study, however, despite lower food intake and similar energy intake, mice fed HFD (189% of energy from fat) for 16 weeks gained more body weight and body fat than mice fed LFD (42% of energy from fat), which provided more energy as carbohydrate (sugar and maize starch). This is consistent with a previous finding that body weight and adiposity, but not energy intake, increased in HFD-fed C57BL/6J mice compared with LFD-fed mice during the first 17 weeks of feeding, although energy intake was significantly higher in HFD-fed mice after 17 weeks owing to a reduction in leptin sensitivity⁽²⁰⁾. Body weight is normally maintained by a balance between energy intake and energy expenditure. When energy intake exceeds energy expenditure, excess energy is stored as TAG in the adipose tissue, resulting in overweight

or obesity. Because energy expenditure during dark hours was significantly lower in HFD-fed mice than in LFD-fed mice, the increase in body weight and fat mass in HFD-fed mice may be due to a positive energy balance resulting from a decrease in energy expenditure relative to energy intake.

Induction of energy expenditure based on fatty acid oxidation in WAT may reduce adiposity⁽²¹⁾. Mitochondrial biogenesis and thermogenesis are decreased in WAT of obese individuals and rodents^(21–23), while induction of mitochondria and activation of fatty acid oxidation have been observed in WAT under conditions promoting loss of adiposity⁽²¹⁾. Kusminski and Scherer⁽²⁴⁾ suggested that in the obese state, mitochondria in WAT cannot cope with increasing demands for fatty acid oxidation, resulting in incomplete β -oxidation. In the present study, HFD down-regulated the expression of genes involved in fatty acid catabolism and oxidation, as well as genes controlling the mitochondrial energy transduction pathways, including the TCA cycle and oxidative phosphorylation, in the epididymal WAT. In other studies, expression of *Faah* (a catabolic gene for bioactive fatty acid amides) in adipose tissue was negatively correlated with visceral fat mass in human subjects⁽²⁵⁾, and mice lacking *Faah* had increased body weight and fat mass with decreased energy expenditure⁽²⁶⁾. Thus, down-regulation of genes regulating fatty acid catabolism, fatty acid oxidation and energy metabolism in epididymal WAT may be partly responsible for the decrease in energy expenditure induced by HFD. Our findings also suggest that the deleterious effects of HFD on adipose tissue mitochondria are associated with decreased expression of genes involved in antioxidant defence and detoxification. An altered redox state is associated with the accumulation of products of incomplete β -oxidation and increased mitochondrial reactive oxygen species formation, leading to a

Table 4. Fold changes of selected genes influenced by high-fat diet*

Up-regulated genes			Down-regulated genes		
Symbol	Fold change	<i>P</i>	Symbol	Fold change	<i>P</i>
Chemokines and their receptors			Oxidation–reduction		
<i>Ccl2</i>	3.08	3.62×10^{-04}	<i>Gpx3</i>	–2.36	0.002
<i>Ccl3</i>	2.62	8.21×10^{-05}	<i>Aldh1a1</i>	–2.19	0.001
<i>Ccl4</i>	3.37	1.66×10^{-04}	<i>Aldh6a1</i>	–2.31	0.001
<i>Ccl6</i>	3.74	5.73×10^{-05}	<i>Cyp2d9</i>	–3.45	0.011
<i>Ccl7</i>	3.10	5.93×10^{-04}	<i>Cyp2d22</i>	–2.93	0.001
<i>Ccl9</i>	5.34	2.64×10^{-06}	<i>Cyp2e1</i>	–4.69	0.006
<i>Cxcl2</i>	2.04	4.86×10^{-05}	<i>Cyp2f2</i>	–4.42	3.28×10^{-04}
<i>Cxcl12</i>	2.10	9.45×10^{-05}	<i>Gsta3</i>	–2.32	3.48×10^{-05}
<i>Cxcl14</i>	2.03	0.003197	<i>Gsta4</i>	–3.90	3.02×10^{-05}
<i>Cxcl16</i>	2.17	4.72×10^{-05}	<i>Por</i>	–2.19	2.13×10^{-04}
<i>Ccr5</i>	6.00	1.28×10^{-05}	<i>Ndufb4</i>	–2.02	3.24×10^{-04}
<i>Cxcr4</i>	2.94	1.19×10^{-04}	<i>Ndufb9</i>	–2.36	3.89×10^{-04}
Cytokine and trigger receptors			Lipolysis and fatty acid metabolism		
<i>Il7r</i>	15.01	1.03×10^{-06}	<i>Adrb3</i>	–3.78	0.005127
<i>Trem2</i>	31.19	7.63×10^{-07}	<i>Fabp4</i>	–9.01	7.63×10^{-07}
Toll-like receptors			<i>Cd36</i>	–3.58	2.93×10^{-06}
<i>Tlr1</i>	4.28	3.36×10^{-05}	<i>Slc27a2</i>	–2.42	0.032965
<i>Tlr2</i>	2.53	9.58×10^{-05}	<i>Elovl6</i>	–2.61	0.046248
<i>Tlr6</i>	2.44	4.27×10^{-04}	<i>Acsm3</i>	–12.76	2.34×10^{-04}
<i>Tlr7</i>	2.76	5.96×10^{-04}	<i>Faah</i>	–2.04	0.015
<i>Tlr8</i>	5.96	3.86×10^{-05}	<i>Acacb</i>	–4.12	0.001
<i>Tlr13</i>	14.84	1.27×10^{-06}	<i>Acot4</i>	–3.61	0.002
<i>Tlr7</i>	2.76	5.96×10^{-04}	<i>Acadslb</i>	–2.08	0.002
C-type lectin receptors			<i>Hadh</i>	–2.73	8.72×10^{-06}
<i>Clec4a1</i>	2.52	7.61×10^{-05}	Insulin sensitivity		
<i>Clec4a3</i>	3.81	1.20×10^{-05}	<i>Irs2</i>	–2.78	0.005
<i>Clec4b1</i>	4.96	1.40×10^{-05}	<i>Slc2a3</i>	–3.05	1.40×10^{-05}
<i>Clec4d</i>	9.98	6.35×10^{-05}	Skeletal system development and pattern specification process		
<i>Clec7a</i>	5.84	9.06×10^{-06}	<i>Bmp4</i>	–2.54	0.001
<i>Clecsf12</i>	8.02	8.64×10^{-06}	<i>Hoxa5</i>	–2.21	5.21×10^{-05}
Fc receptors			<i>Hoxa7</i>	–2.55	7.07×10^{-05}
<i>Fcgr1</i>	3.44	2.28×10^{-04}	<i>Hoxb5</i>	–2.31	0.001
<i>Fcgr3</i>	6.26	5.97×10^{-06}	<i>Hoxc6</i>	–2.09	4.92×10^{-04}
<i>Fcgr4</i>	4.74	1.75×10^{-04}	<i>Irx3</i>	–2.33	0.004
<i>Fcer1a</i>	2.46	4.63×10^{-04}	<i>Igf2</i>	–2.60	2.26×10^{-04}
<i>Fcer1g</i>	5.51	7.18×10^{-06}	<i>Mmp9</i>	–2.18	2.38×10^{-05}
Surface markers of immune cells			G-protein-coupled receptors and others		
<i>Cd9</i>	4.06	1.56×10^{-05}	<i>Gpr64</i>	–2.85	0.02
<i>Cd14</i>	2.26	6.79×10^{-04}	<i>Gpr120</i>	–2.83	4.81×10^{-04}
<i>Cd44</i>	8.35	2.49×10^{-06}	<i>Gpr109a</i>	–2.57	0.002
<i>Cd53</i>	4.75	2.21×10^{-05}	<i>Gpr156</i>	–2.19	1.13×10^{-04}
<i>Cd63</i>	2.12	5.20×10^{-05}	<i>Opn3</i>	–2.29	0.001
<i>Cd68</i>	15.72	7.85×10^{-07}	<i>Adam7</i>	–2.220	0.04
<i>Cd72</i>	9.73	6.30×10^{-06}			
<i>Cd83</i>	4.14	1.90×10^{-04}			
<i>Cd84</i>	12.41	4.04×10^{-06}			
<i>Cd93</i>	2.04	1.08×10^{-04}			
<i>Cd180</i>	5.92	1.24×10^{-05}			
<i>Cd248</i>	2.09	0.001			
ECM components					
<i>Col1a1</i>	4.71	5.66×10^{-05}			
<i>Col3a1</i>	2.64	8.51×10^{-05}			
<i>Col5a2</i>	2.65	5.99×10^{-05}			
<i>Col6a2</i>	2.42	0.001966			
<i>Col6a3</i>	2.39	7.15×10^{-05}			
<i>Sdcbp</i>	2.95	4.74×10^{-05}			
<i>Lum</i>	4.80	1.23×10^{-05}			
<i>Mfap5</i>	2.71	0.001			
<i>Gpnm5</i>	31.53	8.61×10^{-07}			
<i>Fn1</i>	2.58	0.001236			
<i>Itgad</i>	17.29	7.85×10^{-07}			
<i>Itgam</i>	2.00	8.15×10^{-04}			
<i>Itgax</i>	3.37	7.06×10^{-05}			
ECM remodelling and regulation					
<i>Ctsa</i>	4.16	7.96×10^{-07}			

Table 4. Continued

Up-regulated genes			Down-regulated genes		
Symbol	Fold change	P	Symbol	Fold change	P
<i>Ctsh</i>	2.52	4.81×10^{-05}			
<i>Ctsk</i>	13.18	7.85×10^{-07}			
<i>Ctsl</i>	4.14	6.47×10^{-05}			
<i>Ctss</i>	4.93	5.89×10^{-05}			
<i>Ctsz</i>	3.23	8.17×10^{-05}			
<i>Adam8</i>	6.87	1.33×10^{-05}			
<i>Adam12</i>	2.12	2.89×10^{-04}			
<i>Adam17</i>	2.37	4.86×10^{-05}			
<i>Mmp2</i>	4.02	2.16×10^{-05}			
<i>Mmp3</i>	4.17	2.91×10^{-05}			
<i>Mmp12</i>	31.86	1.97×10^{-05}			
<i>Mmp13</i>	3.44	1.95×10^{-05}			
<i>Timp1</i>	7.90	4.74×10^{-05}			
<i>Tgfb1</i>	2.64	1.20×10^{-04}			
Regulator of G protein signalling					
<i>Rgs1</i>	33.98	5.75×10^{-07}			
<i>Rgs10</i>	3.58	3.03×10^{-05}			

* Differentially expressed genes were determined using Limma in R/Bioconductor, based on $P < 0.05$, false discovery rate $< 5\%$ and \log_2 fold change > 1 . For definition of gene abbreviations, see online Supplementary Table S1.

deterioration of insulin sensitivity⁽²⁷⁾. Mitochondrial reactive oxygen species produced by redox imbalance may promote adipocyte differentiation⁽²⁸⁾. In adipose tissue of obese mice such as KKAY mice and HFD-induced obese mice, reactive oxygen species production was accompanied by decreased expression of antioxidant enzymes⁽²⁹⁾.

In the present study, another candidate gene for controlling energy expenditure is the bone morphogenetic protein 4 (*Bmp4*) gene. Recently, Qian *et al.*⁽³⁰⁾ reported that adipose-specific overexpression of *Bmp4* led to reduced body fat mass and increased energy expenditure, whereas *Bmp4*-deficient mice exhibited increased adiposity and impaired

insulin sensitivity, which suggests that *Bmp4* can regulate WAT remodelling and induction of brown adipocyte-like cell structure and function. Interestingly, along with *Bmp4*, multiple genes involved in skeletal system development and pattern specification were down-regulated in the present study. Similarly, down-regulation of homeobox genes, including *Hoxa5*, was observed in the epididymal WAT of ob/ob mice compared with lean controls⁽³¹⁾, whereas expression of homeobox genes (e.g. *Hoxa5*, *Hoxb5*, *Hoxc6* and *Irx3*) was up-regulated after fat loss in human subjects⁽³²⁾. Recently, Gehrke *et al.*⁽³³⁾ suggested epigenetic regulation, in particular DNA methylation of *HOX* genes as a mechanism that explains

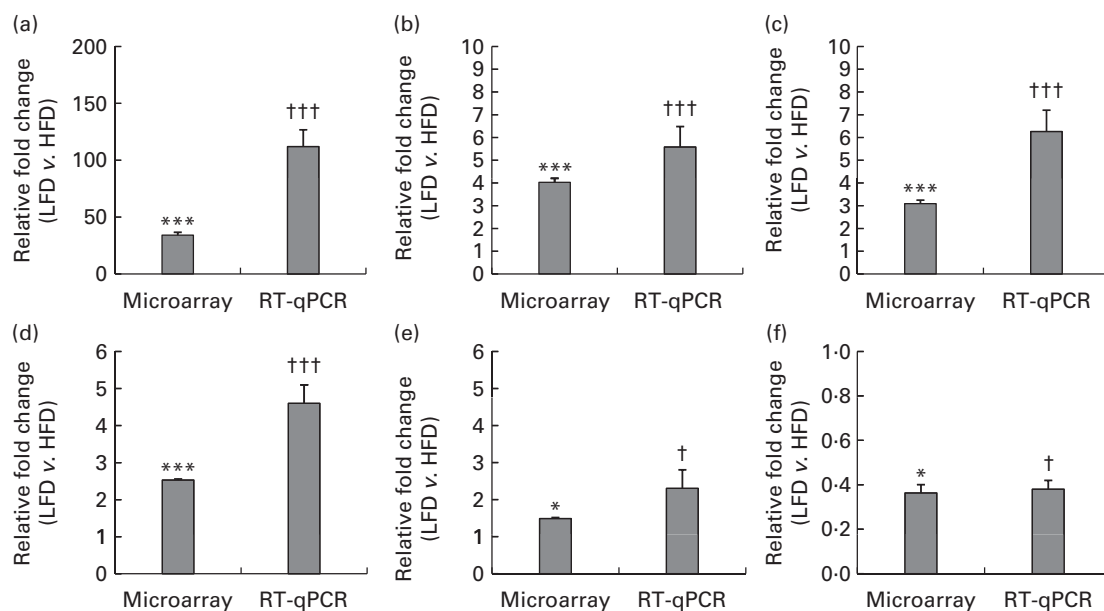


Fig. 2. Validation of microarray data using real-time quantitative PCR (RT-qPCR) for (a) *Rgs1*, (b) *Mmp2*, (c) *Ccl2*, (d) *Tlr2*, (e) *Tlr4* and (f) *Irs2*. Values are means with their standard errors represented by vertical bars. * $P < 0.05$, *** $P < 0.001$ (Wilcoxon *t* test). † $P < 0.05$, ††† $P < 0.001$ (Student's *t* test). LFD, low-fat diet; HFD, high-fat diet. For definition of gene abbreviations, see online Supplementary Table S1.



how these transcriptional factors exhibit such a distinct depot-specific expression pattern. Different adipose depots are known to mediate different effects on the risk for metabolic disorders⁽³³⁾. Moreover, obese patients with type 2 diabetes had lower expression of *Igf2* in the adipose tissue compared with those who were lean⁽³⁴⁾, and down-regulation of *Igf2* in the adipose tissue contributed to the paternal transmission of HFD-induced obesity⁽³⁵⁾. However, many genes related to skeletal system development and pattern specification still have unknown roles in the development of obesity. Thus, understanding these genes will facilitate the development of novel approaches in the treatment of obesity.

In contrast, since the NEFA released by lipolysis or taken up by cells can be utilised in WAT as a source of energy through β -oxidation in the mitochondria, a decrease in the expression of genes involved in lipolysis and fatty acid uptake and transport in response to HFD may reduce β -oxidation, resulting in excessive fat accumulation. In mice, *Adrb3* disruption reduces lipolysis and increases body fat accumulation⁽³⁶⁾, and *Adrb3* increases thermogenesis in the brown adipose tissue⁽³⁷⁾. Deficiency of *Fabp4* also reduces lipolysis in mice⁽³⁸⁾, and a decrease in *Fabp4* expression in the adipose tissue has been found to be inversely associated with obesity in human subjects⁽³⁹⁾.

The expression of several GPCR genes, including *Gpr64*, *Gpr120*, *Gpr109a*, *Gpr156* and *Opn3*, was down-regulated by HFD in the present study. Mice lacking *Gpr120*, an NEFA-sensing GPCR, exhibited obesity, glucose intolerance and fatty liver⁽⁴⁰⁾. Furthermore, *Gpr109a* has been reported to act as a metabolic sensor activated by intermediates of energy metabolism, and its expression was down-regulated in the adipose tissue of HFD-fed mice⁽⁴¹⁾. In contrast, the expression of genes encoding RGS (*Rgs1* and *Rgs10*) was up-regulated by HFD. The RGS family is involved in the rapid turn-off of GPCR signalling pathways⁽⁴²⁾. Huang *et al.*⁽⁴³⁾ demonstrated that RGS-insensitive *Gai2G184S* mice exhibited resistance to the metabolic effects of HFD, and were protected from insulin resistance by increasing energy expenditure and peripheral insulin sensitivity. Furthermore, in another study, *Rgs2*- and *Rgs5*-deficient mice had less body mass and body fat than littermate controls^(44,45). However, the specific roles of most GPCR and RGS genes in the adipose tissue are not yet fully understood.

Obesity is characterised by extensive reorganisation of the adipose tissue, which involves ECM remodelling and adipogenesis⁽⁴⁶⁾. Cathepsins, ADAM, MMP and their inhibitors (i.e. TIMP) are involved in ECM remodelling⁽⁴⁷⁾. The present study indicated that mRNA levels of most genes involved in ECM remodelling were up-regulated in obese adipose tissues compared with lean tissues, while expression of *Adam7* and *Mmp9* was down-regulated in obesity. Interestingly, mice lacking *Ctsk*, *Ctsl*, *Adam12*, *Timp1* or *Mmp2*, but not *Mmp9*, were protected against obesity^(48–53). Belo *et al.*⁽⁵⁴⁾ reported the association between *Mmp9* gene polymorphisms and lower plasma *Mmp9* level in obese children and adolescents, suggesting a potential role of *Mmp9* gene in the development of obesity. We also observed that HFD up-regulated the expression of *Tgfb1* (encoding a profibrotic cytokine), as

well as genes encoding various ECM components, including members of the collagen family, and increased adipose collagen accumulation, suggesting that HFD may facilitate abnormal ECM accumulation in WAT, promoting fibrosis. In addition, we detected significant expression of genes for a lymphocyte chemotactic factor (*Cxcl12*) and its receptor (*Cxcr4*), as well as genes related to macrophage infiltration (*Ccl2*, *Cxcl14* and *Ccr5*) in WAT of HFD-fed mice. It is well known that macrophage infiltration plays a critical role in adipose tissue inflammation, and that chemokines are involved in this process. In obese mice, a deficiency of *Ccl2*, *Cxcl14* or *Ccr5* decreased macrophage infiltration in the adipose tissue and improved metabolic function, while overexpression of *Ccl2* in the adipose tissue caused the opposite phenotype^(55–58). Besides macrophages, T and B lymphocytes have been shown to accumulate in the adipose tissue of obese mice and have been associated with inflammation and insulin resistance^(59,60).

Many other genes involved in innate or adaptive immune and inflammatory responses, such as those encoding toll-like receptors, C-type lectin receptors, Fc receptors, cytokine receptors and triggering receptors, were up-regulated by HFD. One of these genes, *Tlr2*, has been associated with increased adiposity, macrophage infiltration and inflammatory cytokine expression⁽⁶¹⁾. *Saa3*, which encodes an inflammatory adipocytokine and may be a potential link between obesity and its metabolic complications⁽⁶²⁾, was also one of the top ten genes up-regulated by HFD in the present study. However, despite the increased expression of multiple inflammatory genes in WAT of HFD-fed mice, plasma concentrations of inflammatory chemokines and cytokines were not affected, as described in a previous study⁽⁶³⁾. Thomas *et al.*⁽⁶³⁾ suggested that shifts in these inflammation markers in the blood are probably not as sensitive as WAT mRNA patterns, which reflect the inflammatory status of the local tissue.

Tph2, *Ubd* and *Atf3* were also among the genes most highly up-regulated by HFD in the present study. Although a deficiency of *Tph2* or *Ubd* in mice caused body fat reduction by increasing energy expenditure^(64,65), the specific functions of these genes in the adipose tissue are still unclear. *Atf3* has been reported to act as a negative regulator of SFA/TLR4 signalling and macrophage activation in obese adipose tissue⁽⁶⁶⁾; however, overexpression of *Atf3* decreased mitochondrial function and mitochondria-related gene expression in adipocytes *in vivo* and *in vitro*⁽⁶⁷⁾. Thus, further experiments are required to evaluate whether *Atf3* has a beneficial or detrimental role in obesity and its associated metabolic disturbances.

In conclusion, long-term HFD feeding predominantly up-regulated a series of genes involved in immune and inflammatory responses, as well as cell activation and division in WAT of C57BL/6J mice. Genes down-regulated by HFD were mainly implicated in fatty acid metabolism, oxidation–reduction, insulin response and skeletal system development. The top ten up-regulated genes were *Rgs1*, *Mmp12*, *Gpnmb*, *Trem2*, *Tph2*, *Saa3*, *Ubd*, *Atf3*, *Itgad* and *Cd68*, which might be associated with energy expenditure (*Rgs1*, *Tph2*, *Ubd* and *Atf3*), ECM remodelling and components (*Mmp12*, *Gpnmb*

and *Itgad*) and inflammation (*Trem2*, *Saa3*, *Atf3* and *Cd68*); further studies are needed to evaluate the roles of these genes in the pathophysiology of the adipose tissue. The functions of the top ten down-regulated genes, except *Pck* and *Fabp4*, are also poorly understood. Thus, the present findings will be useful in future efforts to identify the therapeutic targets for obesity. However, further studies are needed to investigate the molecular mechanisms responsible for WAT depot-specific differences.

Supplementary material

To view supplementary material for this article, please visit <http://dx.doi.org/10.1017/S0007114515000100>

Acknowledgements

The present study was supported by the Basic Science Research Program (U. J. J., grant no. NRF-2011-0022387, NRF-2014R1A1A4A01007858), the SRC program (M.-S. C., Center for Food & Nutritional Genomics, grant no. 2008-0062618) and the fundamental technology program (M.-S. C., grant no. 2012M3A9C4048818) of the National Research Foundation of Korea funded by the Ministry of Education, Science and Technology. This study received no specific grant from any funding agency, commercial or not-for-profit sectors. In addition, all the funders had no role in the design and analysis of the study or in the writing of this article.

The authors' contributions are as follows:

M.-S. C. designed the study and participated in the writing of the manuscript; Y.-J. K. performed the animal experiments; J. Y. R. and S. R. K. were involved in data interpretation and edited the manuscript; U. J. J. analysed the data and wrote the manuscript. All authors read and approved the final manuscript.

The authors declare that there is no conflict of interest.

References

- Jung UJ & Choi MS (2014) Obesity and its metabolic complications: the role of adipokines and the relationship between obesity, inflammation, insulin resistance, dyslipidemia and nonalcoholic fatty liver disease. *Int J Mol Sci* **15**, 6184–6223.
- Rolls BJ & Hammer VA (1995) Fat, carbohydrate, and the regulation of energy intake. *Am J Clin Nutr* **62**, 1086S–1095S.
- Savastano DM & Covasa M (2005) Adaptation to a high-fat diet leads to hyperphagia and diminished sensitivity to cholecystokinin in rats. *J Nutr* **135**, 1953–1959.
- Buettner R, Newgard CB, Rhodes CJ, *et al.* (2000) Correction of diet-induced hyperglycemia, hyperinsulinemia, and skeletal muscle insulin resistance by moderate hyperleptinemia. *Am J Physiol Endocrinol Metab* **278**, E563–E569.
- Leibowitz SF, Dourmashkin JT, Chang GQ, *et al.* (2004) Acute high-fat diet paradigms link galanin to triglycerides and their transport and metabolism in muscle. *Brain Res* **1008**, 168–178.
- Do GM, Oh HY, Kwon EY, *et al.* (2011) Long-term adaptation of global transcription and metabolism in the liver of high-fat diet-fed C57BL/6J mice. *Mol Nutr Food Res* **55**, S173–S185.
- Kalupahana NS, Voy BH, Saxton AM, *et al.* (2011) Energy-restricted high-fat diets only partially improve markers of systemic and adipose tissue inflammation. *Obesity (Silver Spring)* **19**, 245–254.
- Oscari LB, Miller WC & Arnall DA (1987) Effects of dietary sugar and of dietary fat on food intake and body fat content in rats. *Growth* **51**, 64–73.
- Hulman S & Falkner B (1994) The effect of excess dietary sucrose on growth, blood pressure, and metabolism in developing Sprague–Dawley rats. *Pediatr Res* **36**, 95–101.
- Santos FL, Esteves SS, da Costa Pereira A, *et al.* (2012) Systematic review and meta-analysis of clinical trials of the effects of low carbohydrate diets on cardiovascular risk factors. *Obes Rev* **13**, 1048–1066.
- Ruth MR, Port AM, Shah M, *et al.* (2013) Consuming a hypocaloric high fat low carbohydrate diet for 12 weeks lowers C-reactive protein, and raises serum adiponectin and high density lipoprotein-cholesterol in obese subjects. *Metabolism* **62**, 1779–1787.
- Hageman RS, Wagener A, Hantschel C, *et al.* (2010) High-fat diet leads to tissue-specific changes reflecting risk factors for diseases in DBA/2J mice. *Physiol Genomics* **42**, 55–66.
- Bjørndal B, Burri L, Staalesen V, *et al.* (2011) Different adipose depots: their role in the development of metabolic syndrome and mitochondrial response to hypolipidemic agents. *J Obes* **2011**, 490650.
- Chau YY, Bandiera R, Serrels A, *et al.* (2014) Visceral and subcutaneous fat have different origins and evidence supports a mesothelial source. *Nat Cell Biol* **16**, 367–375.
- Briones AM, Nguyen Dinh Cat A, Callera GE, *et al.* (2012) Adipocytes produce aldosterone through calcineurin-dependent signaling pathways: implications in diabetes mellitus-associated obesity and vascular dysfunction. *Hypertension* **59**, 1069–1078.
- Xu H, Barnes GT, Yang Q, *et al.* (2003) Chronic inflammation in fat plays a crucial role in the development of obesity-related insulin resistance. *J Clin Invest* **112**, 1821–1830.
- Altintas MM, Azad A, Nayer B, *et al.* (2011) Mast cells, macrophages, and crown-like structures distinguish subcutaneous from visceral fat in mice. *J Lipid Res* **52**, 480–488.
- Liu LF, Shen WJ, Ueno M, *et al.* (2013) Age-related modulation of the effects of obesity on gene expression profiles of mouse bone marrow and epididymal adipocytes. *PLOS ONE* **8**, e72367.
- Do GM, Kwon EY, Kim E, *et al.* (2010) Hepatic transcription response to high-fat treatment in mice: microarray comparison of individual vs. pooled RNA samples. *Biotechnol J* **5**, 970–973.
- Lin S, Thomas TC, Storlien LH, *et al.* (2000) Development of high fat diet-induced obesity and leptin resistance in C57BL/6J mice. *Int J Obes Relat Metab Disord* **24**, 639–646.
- Flachs P, Rossmeisl M, Kuda O, *et al.* (2013) Stimulation of mitochondrial oxidative capacity in white fat independent of UCP1: a key to lean phenotype. *Biochim Biophys Acta* **1831**, 986–1003.
- Valerio A, Cardile A, Cozzi V, *et al.* (2006) TNF-alpha down-regulates eNOS expression and mitochondrial biogenesis in fat and muscle of obese rodents. *J Clin Invest* **116**, 2791–2798.
- Böttcher H & Fürst P (1997) Decreased white fat cell thermogenesis in obese individuals. *Int J Obes Relat Metab Disord* **21**, 439–444.

24. Kusminski CM & Scherer PE (2012) Mitochondrial dysfunction in white adipose tissue. *Trends Endocrinol Metab* **23**, 435–443.
25. Blüher M, Engeli S, Klöting N, *et al.* (2006) Dysregulation of the peripheral and adipose tissue endocannabinoid system in human abdominal obesity. *Diabetes* **55**, 3053–3060.
26. Vaitheesvaran B, Yang L, Hartil K, *et al.* (2012) Peripheral effects of FAAH deficiency on fuel and energy homeostasis: role of dysregulated lysine acetylation. *PLOS ONE* **7**, e33717.
27. Muoio DM & Neuffer PD (2012) Lipid-induced mitochondrial stress and insulin action in muscle. *Cell Metab* **15**, 595–605.
28. Tormos KV, Anso E, Hamanaka RB, *et al.* (2011) Mitochondrial complex III ROS regulate adipocyte differentiation. *Cell Metab* **14**, 537–544.
29. Furukawa S, Fujita T, Shimabukuro M, *et al.* (2004) Increased oxidative stress in obesity and its impact on metabolic syndrome. *J Clin Invest* **114**, 1752–1761.
30. Qian SW, Tang Y, Li X, *et al.* (2013) BMP4-mediated brown fat-like changes in white adipose tissue alter glucose and energy homeostasis. *Proc Natl Acad Sci U S A* **110**, E798–E807.
31. Yamamoto Y, Gesta S, Lee KY, *et al.* (2010) Adipose depots possess unique developmental gene signatures. *Obesity (Silver Spring)* **18**, 872–878.
32. Dankel SN, Fadnes DJ, Stavrum AK, *et al.* (2010) Switch from stress response to homeobox transcription factors in adipose tissue after profound fat loss. *PLoS ONE* **5**, e11033.
33. Gehrke S, Brueckner B, Schepky A, *et al.* (2013) Epigenetic regulation of depot-specific gene expression in adipose tissue. *PLOS ONE* **8**, e82516.
34. Chen M, Macpherson A, Owens J, *et al.* (2012) Obesity alone or with type 2 diabetes is associated with tissue specific alterations in DNA methylation and gene expression of *PPARGC1A* and *IGF2*. *J Diabetes Res Clin Metab* **1**, 1–8.
35. Morita S, Horii T, Kimura M, *et al.* (2014) Paternal allele influences high fat diet-induced obesity. *PLOS ONE* **9**, e85477.
36. Revelli JP, Preitner F, Samec S, *et al.* (1997) Targeted gene disruption reveals a leptin-independent role for the mouse beta3-adrenoceptor in the regulation of body composition. *J Clin Invest* **100**, 1098–1106.
37. Arner P & Hoffstedt J (1999) Adrenoceptor genes in human obesity. *J Intern Med* **245**, 667–672.
38. Scheja L, Makowski L, Uysal KT, *et al.* (1999) Altered insulin secretion associated with reduced lipolytic efficiency in *aP2^{-/-}* mice. *Diabetes* **48**, 1987–1994.
39. Queipo-Ortuño MI, Escoté X, Ceperuelo-Mallafre V, *et al.* (2012) FABP4 dynamics in obesity: discrepancies in adipose tissue and liver expression regarding circulating plasma levels. *PLOS ONE* **7**, e48605.
40. Ichimura A, Hirasawa A, Poulain-Godefroy O, *et al.* (2012) Dysfunction of lipid sensor GPR120 leads to obesity in both mouse and human. *Nature* **483**, 350–354.
41. Wanders D, Graff EC & Judd RL (2012) Effects of high fat diet on *GPR109A* and *GPR81* gene expression. *Biochem Biophys Res Commun* **425**, 278–283.
42. De Vries L, Zheng B, Fischer T, *et al.* (2000) The regulator of G protein signaling family. *Annu Rev Pharmacol Toxicol* **40**, 235–271.
43. Huang X, Charbeneau RA, Fu Y, *et al.* (2008) Resistance to diet-induced obesity and improved insulin sensitivity in mice with a regulator of G protein signaling-insensitive G184S *Gnai2* allele. *Diabetes* **57**, 77–85.
44. Cho H, Park C, Hwang IY, *et al.* (2008) *Rgs5* targeting leads to chronic low blood pressure and a lean body habitus. *Mol Cell Biol* **28**, 2590–2597.
45. Nunn C, Zhao P, Zou MX, *et al.* (2011) Resistance to age-related, normal body weight gain in *RGS2* deficient mice. *Cell Signal* **23**, 1375–1386.
46. Crandall DL, Hausman GJ & Kral JG (1997) A review of the microcirculation of adipose tissue: anatomic, metabolic, and angiogenic perspectives. *Microcirculation* **4**, 211–232.
47. Järveläinen H, Sainio A, Koulu M, *et al.* (2009) Extracellular matrix molecules: potential targets in pharmacotherapy. *Pharmacol Rev* **61**, 198–223.
48. Lijnen HR, Demeulemeester D, Van Hoef B, *et al.* (2003) Deficiency of tissue inhibitor of matrix metalloproteinase-1 (TIMP-1) impairs nutritionally induced obesity in mice. *Thromb Haemost* **89**, 249–255.
49. Masaki M, Kurisaki T, Shirakawa K, *et al.* (2005) Role of meltrin [alpha] (*ADAM12*) in obesity induced by high-fat diet. *Endocrinology* **146**, 1752–1763.
50. Van Hul M & Lijnen HR (2008) A functional role of gelatinase A in the development of nutritionally induced obesity in mice. *J Thromb Haemost* **6**, 1198–1206.
51. Yang M, Zhang Y, Pan J, *et al.* (2007) Cathepsin L activity controls adipogenesis and glucose tolerance. *Nat Cell Biol* **9**, 970–977.
52. Yang M, Sun J, Zhang T, *et al.* (2008) Deficiency and inhibition of cathepsin K reduce body weight gain and increase glucose metabolism in mice. *Arterioscler Thromb Vasc Biol* **28**, 2202–2208.
53. Van Hul M, Piccard H & Lijnen HR (2010) Gelatinase B (*MMP-9*) deficiency does not affect murine adipose tissue development. *Thromb Haemost* **104**, 165–171.
54. Belo VA, Souza-Costa DC, Luizon MR, *et al.* (2012) Matrix metalloproteinase-9 genetic variations affect *MMP-9* levels in obese children. *Int J Obes (Lond)* **36**, 69–75.
55. Kanda H, Tateya S, Tamori Y, *et al.* (2006) *MCP-1* contributes to macrophage infiltration into adipose tissue, insulin resistance, and hepatic steatosis in obesity. *J Clin Invest* **116**, 1494–1505.
56. Kamei N, Tobe K, Suzuki R, *et al.* (2006) Overexpression of monocyte chemoattractant protein-1 in adipose tissues causes macrophage recruitment and insulin resistance. *J Biol Chem* **281**, 26602–26614.
57. Nara N, Nakayama Y, Okamoto S, *et al.* (2007) Disruption of CXC motif chemokine ligand-14 in mice ameliorates obesity-induced insulin resistance. *J Biol Chem* **282**, 30794–30803.
58. Kitade H, Sawamoto K, Nagashimada M, *et al.* (2012) *CCR5* plays a critical role in obesity-induced adipose tissue inflammation and insulin resistance by regulating both macrophage recruitment and M1/M2 status. *Diabetes* **61**, 1680–1690.
59. Kintscher U, Hartge M, Hess K, *et al.* (2008) T-lymphocyte infiltration in visceral adipose tissue: a primary event in adipose tissue inflammation and the development of obesity-mediated insulin resistance. *Arterioscler Thromb Vasc Biol* **28**, 1304–1310.
60. Winer DA, Winer S, Shen L, *et al.* (2011) B cells promote insulin resistance through modulation of T cells and production of pathogenic IgG antibodies. *Nat Med* **17**, 610–617.
61. Himes RW & Smith CW (2010) *Tlr2* is critical for diet-induced metabolic syndrome in a murine model. *FASEB J* **24**, 731–739.
62. Yang RZ, Lee MJ, Hu H, *et al.* (2006) Acute-phase serum amyloid A: an inflammatory adipokine and potential link between obesity and its metabolic complications. *PLoS Med* **3**, 884–894.
63. Thomas AP, Dunn TN, Oort PJ, *et al.* (2011) Inflammatory phenotyping identifies *CD11d* as a gene markedly induced



- in white adipose tissue in obese rodents and women. *J Nutr* **141**, 1172–1180.
64. Yadav VK, Oury F, Suda N, *et al.* (2009) A serotonin-dependent mechanism explains the leptin regulation of bone mass, appetite, and energy expenditure. *Cell* **138**, 976–989.
 65. Canaan A, Defuria J, Perelman E, *et al.* (2014) Extended lifespan and reduced adiposity in mice lacking the *FAT10* gene. *Proc Natl Acad Sci U S A* **111**, 5313–5318.
 66. Suganami T, Yuan X, Shimoda Y, *et al.* (2009) Activating transcription factor 3 constitutes a negative feedback mechanism that attenuates saturated fatty acid/toll-like receptor 4 signaling and macrophage activation in obese adipose tissue. *Circ Res* **105**, 25–32.
 67. Jang MK, Son Y & Jung MH (2013) ATF3 plays a role in adipocyte hypoxia-mediated mitochondria dysfunction in obesity. *Biochem Biophys Res Commun* **431**, 421–427.